Energy-Transfer Rate in Crystals of Double-Complex Salts Composed of $[Ru(N\text{-}N)_3]^{2+}$ (N-N = 2,2′-Bipyridine or 1,10-Phenanthroline) and $[Cr(CN)_6]^{3-}$: Effect of Relative Orientation between Donor and Acceptor

Takuhiro Otsuka,* Akiko Sekine, Naoki Fujigasaki, Yuji Ohashi, and Youkoh Kaizu*

Department of Chemistry, Tokyo Institute of Technology, O-okayama, Meguro-ku, Tokyo 152-8551, Japan

Received December 11, 2000

A block single-crystal was obtained using a diffusion method with a concentrated acetone−water (vol. 1/1) solution of $[Ru(phen)_3]Cl_2 \cdot 6H_2O$ (phen = 1,10-phenanthroline) and a concentrated aqueous solution of $K_3[Cr(CN)_6]$, without evaporating solvents. The crystal was identified as a double-complex salt including two acetone and fourteen solvent water molecules, $[Ru(phen)_3]_2[Cr(CN)_6]Cl \cdot 2(CH_3)_2CO \cdot 14H_2O$ (**1**). Measurement of the X-ray diffraction pattern of the double-complex salt was performed using an X-ray diffractometer with an Imaging-Plate (IP) Weissenberg camera. **1** crystallizes in the triclinic space group $P\bar{1}$, with $a = 13.930(5)$ Å, $b = 14.783(5)$ Å, $c = 11.137(6)$ Å, $\alpha = 89.87(4)°$, $\beta = 107.47(3)°$, $\gamma = 96.68(3)°$, and $Z = 2$. The crystal structure is very different from that of $[Ru(bpy)_3]_2[Cr(CN)_6]Cl \cdot 8H_2O$ (**2**) (bpy = 2,2′-bipyridine), which could be obtained using the same procedure and crystallizes in the monoclinic space group $C2$, with $a = 22.414(2)$ Å, $b = 13.7686(15)$ Å, $c = 22.207(2)$ Å, $\beta = 90.713(8)°$, and $Z = 4$. The distance between the central-metal ions of ruthenium(II) and chromium(III) complexes in $[Ru(phen)_3]_2[Cr(CN)_6]Cl \cdot 2(CH_3)_2CO \cdot 14H_2O$ (7.170 Å) is shorter than that in $[Ru(bpy)_3]_2[Cr(CN)_6]Cl \cdot 8H_2O$ (9.173 Å) by about 2 Å, while the rate of energy transfer from the ^{3}MLCT state of $[Ru(N\text{-}N)_3]^{2+}$ to the ^2E_g state of $[Cr(CN)_6]^{3-}$ in the former salt (9.5×10^5 s^{-1}) is far slower than that in the latter one (6.0×10^6 s^{-1}) at 77 K. These results indicate that the energy-transfer rate strongly depends, not upon the distance between central metal ions, rather, upon the mutual relative orientation between the donor and the acceptor complexes in double-complex salts.

Introduction

Intermolecular excitation energy transfer between transition-metal complexes in molecular crystals was first studied by Schlöfer et al., who carried out a study between Cr(III) complexes,[1−4] and by Fujita and Kobayashi, who studied the transfer between Ru(II) and Cr(III) complexes.[5−7] Since then, the study of energy transfer between metal complexes had not been an active field compared with that of rare-earth metal ions in ionic crystals,[8] although the distance, relative geometry, and energy gap of excited states between donor and acceptor complexes can be controlled by using various ligands and central metal ions. Recently, study of the energy transfer between metal complexes in crystals has become an active branch in the field of energy transfer.[9−16] In a previous paper,[9] we reported that energy transfer occurs via ^{3}MLCT(Ru) → ^2E_g(Cr) at a very fast rate (7×10^8 s^{-1}) in the double-complex salt, $Na[Ru(bpy)_3][Cr(ox)_3]$ (bpy = 2,2′-bipyridine). The Hauser group has studied energy transfer in single crystals of double-complex salts composed of $[M_I(bpy)_3]^{2+/3+}$ (M_I^{2+} = Ru^{2+}, Os^{2+}; M_I^{3+} = Rh^{3+}) and $[M_{II}(ox)_3]^{3-}$ (M_{II}^{3+} = Al^{3+}, Cr^{3+}).[10−13] They reported resonant and phonon-assisted excitation energy transfer in the R_1 lines of $[Cr(ox)_3]^{3-}$ in $Na[Rh(bpy)_3][Cr(ox)_3]ClO_4$.[11] Moreover, they described the energy transfer from $[Cr(ox)_3]^{3-}$ to $[Cr(bpy)_3]^{3+}$ in $Na[Rh_{0.99}Cr_{0.01}(bpy)_3][Al_{1-x}Cr_x(ox)_3]ClO_4$ (x = 0−1) and $Na[Rh_{1-y}Cr_y(bpy)_{1-y}][Al_{0.99}Cr_{0.01}(ox)_3]ClO_4$ (y = 0−0.05).[12] They concluded that energy transfer occurs by means of two mechanisms: the superexchange coupling between the Cr^{3+} ions via π overlap of oxalate and bipyridine ligands, and a dipole−dipole mechanism. Recently, they determined the critical distance of energy transfer between $[Ru(bpy)_3]^{2+}$ and $[Cr(ox)_3]^{3-}$ and between $[Ru(bpy)_3]^{2+}$ and $[Os(bpy)_3]^{2+}$.[13]

The energy transfer rate depends mainly upon the following three factors: (i) the distance between donor and acceptor, (ii) the spectral overlap between the donor's luminescence and the acceptor's absorption spectra, and (iii) the relative orientation of the donor and the acceptor in relation to each other. In a previous paper,[14] we examined the relationship between the energy-transfer rate and the spectral overlap (factor (ii)) in

* To whom correspondence may be addressed.

(1) Gausmann, H.; Schläfer, H. L. *J. Chem. Phys.* **1968**, *48*, 4056.
(2) Schläfer, H. L.; Gausmann, H.; Möius, C. *Inorg. Chem.* **1969**, *8*, 1137.
(3) Kirk, A. D.; Ludi, A.; Schläfer, H. L. *Ber. Bunsen-Ges.* **1969**, *13*, 669.
(4) Kirk, A. D.; Schläfer, H. L. *J. Chem. Phys.* **1970**, *52*, 2411.
(5) Fujita, I.; Kobayashi, H. *J. Chem. Phys.* **1970**, *52*, 4904.
(6) Fujita, I.; Kobayashi, H. *Ber. Bunsen-Ges.* **1972**, *76*, 115.
(7) Fujita, I.; Kobayashi, H. *J. Chem. Phys.* **1973**, *59*, 2902.
(8) Blasse, G. *Adv. Inorg. Chem.* **1990**, *35*, 319.
(9) Otsuka, T.; Kaizu, Y. *Chem. Lett.* **1997**, 79.
(10) Decurtins, S.; Schmalle, H. W.; Pellaux, R.; Schneuwly, P.; Hauser, A. *Inorg. Chem.* **1996**, *35*, 1451.
(11) von Arx, M. E.; Hauser, A. *Phys. Rev. B*: **1996**, *54*, 15800.
(12) Langford, V. S.; von Arx, M. E.; Hauser, A. *J. Phys. Chem. A* **1999**, *103*, 7161.
(13) von Arx, M. E.; Burattini, E.; Hauser, A. *J. Phys. Chem. A* **2000**, *104*, 883.
(14) Otsuka, T.; Takahashi, N.; Fujigasaki, N.; Sekine, A.; Ohashi, Y.; Kaizu, Y. *Inorg. Chem.* **1999**, *38*, 1340.
(15) Otsuka, T.; Takahashi, N.; Kaizu, Y. *Mol. Cryst. Liq. Cryst.* **1996**, *286*, 269.
(16) Otsuka, T.; Kaizu, Y. In *Reactivity in Molecular Crystals, Kodansha*; Ohashi, Y., Ed.; Tokyo, 1993; Ch 2, p 103.

10.1021/ic0013936 CCC: $20.00
Published on Web 05/31/2001

$[M(bpy)_3]_2[Cr(CN)_6]Cl\cdot 8H_2O$ (M^{2+} = Ru^{2+}, Os^{2+}) by fixing the distance (factor (i)) and relative orientation (factor (iii)) of the two complexes. The crystal and molecular structure of $[Os(bpy)_3]_2[Cr(CN)_6]Cl\cdot 8H_2O$ was determined to be almost the same as that of $[Ru(bpy)_3]_2[Cr(CN)_6]Cl\cdot 8H_2O$ based on X-ray analysis.[14−16] The energy-transfer rate in the former salt (4.9×10^7 s^{-1}) is eight times larger than that in the latter one (6.0×10^6 s^{-1}) at 77 K. This ratio agrees with the ratio of the spectral overlap between the normalized donor's luminescence and the normalized acceptor's absorption (or excitation) spectra. These results show that the energy-transfer rate is directly proportional to the spectral overlap in the double-complex salts which have the same distance and relative orientation between donor and acceptor complexes.

As mentioned above, the path of energy transfer and the effect of spectral overlap upon the rate have been discussed in studies of energy transfer between transition-metal complexes in crystals. However, the geometrical effect between donor and acceptor complexes upon the energy-transfer rate has not yet been discussed.

In the present work, we investigated the relationship between the energy-transfer rate and the relative orientation of donors and acceptors in double-complex salts by maintaining the same spectral overlap (factor (ii)). $[Ru(phen)_3]^{2+}$ (phen = 1,10-phenanthroline) and $[Ru(bpy)_3]^{2+}$ were used as energy donors since both complexes share almost the same luminescence and absorption spectra. Thus, the spectral overlap of $[Ru(phen)_3]^{2+} - [Cr(CN)_6]^{3-}$ is almost the same as that of $[Ru(bpy)_3]^{2+} - [Cr(CN)_6]^{3-}$. The crystal structure of a block single-crystal of $[Ru(phen)_3]_2[Cr(CN)_6]Cl\cdot 2(CH_3)_2CO\cdot 14H_2O$ (triclinic, $P\bar{1}$) was determined by X-ray structure analysis to be very different from that of $[Ru(bpy)_3]_2[Cr(CN)_6]Cl\cdot 8H_2O$ (monoclinic, $C2$). We report herein the effect of the distance and mutual orientation between $[Ru(N-N)_3]^{2+}$ and $[Cr(CN)_6]^{3-}$ upon the energy-transfer rate from $[Ru(N-N)_3]^{2+}$ to $[Cr(CN)_6]^{3-}$ in $[Ru(phen)_3]_2[Cr(CN)_6]Cl\cdot 2(CH_3)_2CO\cdot 14H_2O$ and $[Ru(bpy)_3]_2[Cr(CN)_6]Cl\cdot 8H_2O$.

Experimental Section

Compounds. Single Complex Salts. $[Ru(bpy)_3]Cl_2\cdot 6H_2O$,[6] $[Ru(bpy)_3]Br_2\cdot 6H_2O$,[14] and $K_3[Cr(CN)_6]$[17] were prepared according to a method previously described. $[Ru(phen)_3]Cl_2\cdot 6H_2O$ was prepared by the same procedure as $[Ru(bpy)_3]Cl_2\cdot 6H_2O$, but 1,10-phenanthroline was used instead of 2,2′-bipyridine. These complexes were identified by luminescence and absorption spectra, molar extinction coefficient, and elemental analysis. The values of molar extinction coefficient were within ±5% of the literature's values.

Single Crystals of Double-Complex Salts. Single crystals of double-complex salts composed of $[Ru(N-N)_3]^{2+}$ (N-N = phen, bpy) and $[Cr(CN)_6]^{3-}$ could be obtained by careful layering of a concentrated acetone−water (vol 1/1) solution of $[Ru(N-N)_3]Cl_2\cdot 6H_2O$ on top of a concentrated aqueous solution of $K_3[Cr(CN)_6]$, in a glass cylinder of about 10 mm diameter, and by setting this aside at room temperature for about one week. At this time, the cylinder was sealed in order to prevent the evaporation of acetone. By this method, block crystals whose sizes were a few millimeters were obtained. A single crystal composed of $[Ru(phen)_3]^{2+}$ and $[Cr(CN)_6]^{3-}$ has been identified as a double-complex salt; it includes two acetone molecules and fourteen solvent water molecules, $[Ru(phen)_3]_2[Cr(CN)_6]Cl\cdot 2(CH_3)_2CO\cdot 14H_2O$. In contrast, single crystals of double-complex salts composed of $[Ru(bpy)_3]^{2+}$ and $[Cr(CN)_6]^{3-}$ did not include any acetone molecules whether the cylinder was sealed or not, $[Ru(bpy)_3]_2[Cr(CN)_6]X\cdot 8H_2O$ (X = Cl^-, Br^-).

Measurements. In the measurements of luminescence spectra and luminescence decay curves for the crystals at 77 K, single crystals were used as samples. The measurements were performed as quickly as possible after removing the crystal from the saturated solution, because the double-complex salt $[Ru(phen)_3]_2[Cr(CN)_6]Cl\cdot 2(CH_3)_2CO\cdot 14H_2O$ gradually loses some solvent water and/or acetone molecules into the atmosphere. Luminescence and excitation spectra were measured at 77 K on a Hitachi 850 spectrofluorometer equipped with a Hamamatsu Photonics R928 photomultiplier. The samples were put into a quartz capillary of 3 mm diameter and immersed directly in the coolant (liquid nitrogen). In the capillary, air was substituted with nitrogen gas. Absorption spectra of the aqueous solution were recorded on a Hitachi spectrophotometer model 330 at room temperature. Luminescence decay was recorded on an oscillograph (Lecroy, model 9450) following excitation with the second harmonics (532 nm, fwhm 5 ns) of a Nd:YAG Laser (Spectron, model SL 401). The lifetimes were determined by a semilogarithmic plot of the decay curve. The measurements were performed at least five times with the samples prepared using the same procedure. The luminescence spectra and lifetimes were found to be reproducible within experimental error: ±0.1 nm for the peak maximum of luminescence spectra and ±2% for the lifetime.

Table 1. Summary of Crystallographic Data and Structural Analysis for $[Ru(bpy)_3]_2[Cr(CN)_6]X\cdot 8H_2O$ (X = Cl^-, Br^-) and $[Ru(phen)_3]_2[Cr(CN)_6]Cl\cdot 2(CH_3)_2CO\cdot 14H_2O$

formula	$C_{66}H_{48}ClCrN_{18}O_8Ru_2$	$C_{66}H_{48}BrCrN_{18}O_8Ru_2$	$C_{42}H_{44}Cl_{0.5}Cr_{0.5}N_9O_8Ru$
fw	1510.81	1555.27	947.66
a, Å	22.414	22.414	13.930
b, Å	13.7686	13.814	14.783
c, Å	22.207	22.299	11.137
α, deg	90	90	89.87
β, deg	90.713	90.531	107.47
γ, deg	90	90	96.68
Z	4	4	2
V, Å^3	6852.9	6904.0	2171.4
space group	*C*2	*C*2	*P*1̄
ρ_{calc}, g cm^{-3}	1.464	1.496	1.449
μ, cm^{-1}	6.970	12.32	5.70
T, °C	20	23	23
λ, Å[a]	0.71069	0.71073	0.71073
R[b]	4.89	5.53	11.89
R_w[c]	13.67	9.42	31.6

[a] Radiation, Mo Kα. [b] $R = \sum(|F_o| - |F_c|)/\sum|F_o|$. [c] $R_w = [\sum\{w(F_o^2 - F_c^2)^2\}/\sum\{w(F_o^2)^2\}]^{1/2}$; $w = 1/\{\sigma^2(F_o^2) + (0.2000P)^2\}$; $P = (F_o^2 + 2F_c^2)/3$.

Crystal Structure Determination. Single crystals of $[Ru(bpy)_3]_2[Cr(CN)_6]X\cdot 8H_2O$ (X = Cl^-, Br^-) are stable in the atmosphere at room temperature. Therefore, good accurate diffraction data can be collected using a conventional four-circle diffractometer. In contrast, a single block crystal of $[Ru(phen)_3]_2[Cr(CN)_6]Cl\cdot 2(CH_3)_2CO\cdot 14H_2O$ can easily lose some solvent water and/or acetone molecules into the atmosphere at room temperature. Because the release of some water and/or acetone molecules gradually destroys the crystal lattice of double-complex salt over a few days, good quality diffraction data could not be collected on a conventional four-circle diffractometer. Therefore, in this study, a diffractometer with an Imaging-Plate (IP) Weissenberg camera was used for $[Ru(bpy)_3]_2[Cr(CN)_6]X\cdot 8H_2O$ and $[Ru(phen)_3]_2[Cr(CN)_6]Cl\cdot 2(CH_3)_2CO\cdot 14H_2O$, since the data sets could be collected within 3 h without destroying the crystal lattice. Single-crystal data collection was performed using a Rigaku RAXIS−IIcs imaging-plate system at 296 K, using graphite-monochromatized Mo Kα radiation (λ = 0.71703 Å). The structure was solved using direct methods for $[Ru(bpy)_3]_2[Cr(CN)_6]X\cdot 8H_2O$ and heavy metal methods for $[Ru(phen)_3]_2[Cr(CN)_6]Cl\cdot 2(CH_3)_2CO\cdot 14H_2O$, employing SHELXS-86, and the structures were refined versus F^2 by means of full-matrix least-squares procedures, using SHELXL-93. The data were corrected for Lorentz and polarization factors, but not for absorption or extinction. It is certain that there are no acetone and water molecules between $[Ru(N-N)_3]^{2+}$ and $[Cr(CN)_6]^{3-}$. Details of crystallographic data are listed in Table 1. The selected bond distances and angles are given in Table 2. The ORTEP drawings of the three double-complex salts can be found in the Supporting Information (Figures S-1, S-2, and S-3).

(17) Cruser, F. V. D.; Miller, E. H. *J. Am. Chem. Soc.* **1906**, *28*, 1132.

Table 2. Selected Bond-Length (Å) and Bond-Angle (Deg) in $[Ru(phen)_3]_2[Cr(CN)_6]Cl\cdot 2(CH_3)_2CO\cdot 14H_2O$ (**1**) and $[Ru(bpy)_3]_2[Cr(CN)_6]X\cdot 8H_2O$ ($X^- = Cl^-$ (**2**), Br^- (**3**))

	(**2**)	(**3**)		(**1**)
Cr(1)−C(14)	1.987(13)	2.091(11)	Cr(1)−C(39)	2.078(11)
Cr(1)−C(15)	2.065(12)	2.00(2)	Cr(1)−C(39)#1	2.078(11)
Cr(1)−C(16)	2.066(7)	2.11(2)	Cr(1)−C(37)	2.079(14)
Cr(1)−C(12)	2.076(10)	2.12(2)	Cr(1)−C(37)#1	2.079(14)
Cr(1)−C(11)	2.091(7)	2.104(13)	Cr(1)−C(38)	2.102(12)
Cr(1)−C(13)	2.130(9)	2.00(2)	Cr(1)−C(38)#1	2.102(12)
Ru(1)−N(2B)	2.039(9)	2.002(12)	Ru(1)−N(2)	2.029(8)
Ru(1)−N(3A)	2.053(8)	2.073(12)	Ru(1)−N(4)	2.033(8)
Ru(1)−N(2A)	2.058(7)	2.044(10)	Ru(1)−N(1)	2.040(7)
Ru(1)−N(3B)	2.072(7)	2.062(12)	Ru(1)−N(5)	2.061(10)
Ru(1)−N(4B)	2.077(7)	2.051(11)	Ru(1)−N(6)	2.071(7)
Ru(1)−N(4A)	2.080(6)	2.054(11)	Ru(1)−N(3)	2.081(7)
Ru(2)−N(6B)	2.056(8)	2.072(10)		
Ru(2)−N(7B)	2.058(6)	2.069(12)		
Ru(2)−N(6A)	2.066(7)	2.056(13)		
Ru(2)−N(7A)	2.067(6)	2.097(12)		
Ru(2)−N(5A)	2.084(7)	2.095(9)		
Ru(2)−N(5B)	2.086(7)	2.107(10)		
C(14)−Cr(1)−C(15)	90.2(5)	90.6(7)	C(39)#1−Cr(1)−C(39)	180(0)
C(14)−Cr(1)−C(16)	90.9(4)	90.2(7)	C(39)#1−Cr(1)−C(37)	91.7(4)
C(15)−Cr(1)−C(16)	89.7(3)	90.8(7)	C(39)−Cr(1)−C(37)	88.3(4)
C(14)−Cr(1)−C(12)	92.1(5)	88.6(6)	C(39)#1−Cr(1)−C(37)#1	88.3(4)
C(15)−Cr(1)−C(12)	177.4(6)	178.4(10)	C(39)−Cr(1)−C(37)#1	91.7(4)
C(16)−Cr(1)−C(12)	91.5(3)	90.6(7)	C(37)−Cr(1)−C(37)#1	179.999(2)
C(14)−Cr(1)−C(11)	89.9(4)	177.8(9)	C(39)#1−Cr(1)−C(38)#1	91.5(5)
C(15)−Cr(1)−C(11)	88.6(4)	91.4(7)	C(39)−Cr(1)−C(38)#1	88.5(5)
C(16)−Cr(1)−C(11)	178.1(5)	89.0(6)	C(37)−Cr(1)−C(38)#1	89.5(5)
C(12)−Cr(1)−C(11)	90.2(4)	89.3(6)	C(37)#1−Cr(1)−C(38)#1	90.5(5)
C(14)−Cr(1)−C(13)	179.8(6)	90.6(7)	C(39)#1−Cr(1)−C(38)	88.5(5)
C(15)−Cr(1)−C(13)	89.9(5)	90.9(10)	C(39)−Cr(1)−C(38)	91.5(5)
C(16)−Cr(1)−C(13)	89.1(3)	178.1(9)	C(37)−Cr(1)−C(38)	90.5(5)
C(12)−Cr(1)−C(13)	87.7(4)	87.6(6)	C(37)#1−Cr(1)−C(38)	89.5(5)
C(11)−Cr(1)−C(13)	90.1(4)	90.2(6)	C(38)#1−Cr(1)−C(38)	179.999(2)
N(2B)−Ru(1)−N(3A)	170.0(3)	168.8(5)	N(2)−Ru(1)−N(4)	97.3(4)
N(2B)−Ru(1)−N(2A)	79.7(3)	79.1(4)	N(2)−Ru(1)−N(1)	79.3(3)
N(3A)−Ru(1)−N(2A)	94.2(3)	92.9(4)	N(4)−Ru(1)−N(1)	171.0(3)
N(2B)−Ru(1)−N(3B)	94.0(3)	94.9(5)	N(2)−Ru(1)−N(5)	170.5(3)
N(3A)−Ru(1)−N(3B)	78.6(3)	77.6(5)	N(4)−Ru(1)−N(5)	90.7(4)
N(2A)−Ru(1)−N(3B)	95.5(3)	92.6(5)	N(1)−Ru(1)−N(5)	93.5(3)
N(2B)−Ru(1)−N(4B)	94.9(3)	91.4(5)	N(2)−Ru(1)−N(6)	95.0(4)
N(3A)−Ru(1)−N(4B)	92.3(3)	97.1(5)	N(4)−Ru(1)−N(6)	94.4(3)
N(2A)−Ru(1)−N(4B)	170.1(3)	95.7(5)	N(1)−Ru(1)−N(6)	94.3(3)
N(3B)−Ru(1)−N(4B)	93.1(3)	170.3(5)	N(5)−Ru(1)−N(6)	79.3(4)
N(2B)−Ru(1)−N(4A)	92.3(3)	92.1(5)	N(2)−Ru(1)−N(3)	89.7(3)
N(3A)−Ru(1)−N(4A)	96.0(3)	96.6(4)	N(4)−Ru(1)−N(3)	80.2(3)
N(2A)−Ru(1)−N(4A)	93.4(3)	169.6(5)	N(1)−Ru(1)−N(3)	91.3(3)
N(3B)−Ru(1)−N(4A)	169.9(3)	93.6(4)	N(5)−Ru(1)−N(3)	96.7(3)
N(4B)−Ru(1)−N(4A)	78.4(3)	78.9(4)	N(5)−Ru(1)−N(3)	173.3(3)
N(6B)−Ru(2)−N(7B)	93.1(3)	93.2(4)		
N(6B)−Ru(2)−N(6A)	78.7(3)	79.4(5)		
N(7B)−Ru(2)−N(6A)	93.4(3)	169.4(5)		
N(6B)−Ru(2)−N(7A)	96.2(3)	93.8(4)		
N(7B)−Ru(2)−N(7A)	79.5(3)	79.4(5)		
N(6A)−Ru(2)−N(7A)	171.1(3)	93.4(5)		
N(6B)−Ru(2)−N(5A)	94.1(3)	93.6(4)		
N(7B)−Ru(2)−N(5A)	169.8(3)	95.8(4)		
N(6A)−Ru(2)−N(5A)	95.1(3)	92.3(5)		
N(7A)−Ru(2)−N(5A)	92.6(3)	171.3(5)		
N(6B)−Ru(2)−N(5B)	169.0(3)	170.9(4)		
N(7B)−Ru(2)−N(5B)	95.4(3)	92.7(4)		
N(6A)−Ru(2)−N(5B)	93.9(3)	95.6(5)		
N(7A)−Ru(2)−N(5B)	92.2(3)	94.0(5)		
N(5A)−Ru(2)−N(5B)	78.3(3)	78.9(4)		

Results and Discussion

Crystal Structure and Relative Orientation between $[Ru(N\text{-}N)_3]^{2+}$ and $[Cr(CN)_6]^{3-}$. $[Ru(bpy)_3]_2[Cr(CN)_6]X\cdot 8H_2O$ ($X = Cl^-$, Br^-) crystallize in monoclinic space group *C*2 and have almost the same molecular and crystal structures as $[Os(bpy)_3]_2[Cr(CN)_6]Cl\cdot 8H_2O$.[14] Thus, $[Ru(bpy)_3]_2[Cr(CN)_6]X\cdot 8H_2O$ ($X = Cl^-$, Br^-) have two kinds of $[Ru(bpy)_3]^{2+}$ in the unit cell which are named site-A and site-B. However, both sites have almost the same molecular geometry in the crystals. Each $[Ru(bpy)_3]^{2+}$ in the crystals is found to have as its six nearest neighbors $[Cr(CN)_6]^{3-}$ within 10 Å (9.173−9.883 Å for site-A and 9.244−9.883 Å for site-B). On the other hand, the space group of $[Ru(phen)_3]_2[Cr(CN)_6]Cl\cdot 2(CH_3)_2CO\cdot 14H_2O$ is triclinic $P\bar{1}$. Thus, the geometry of molecules and counter ions around [Ru-

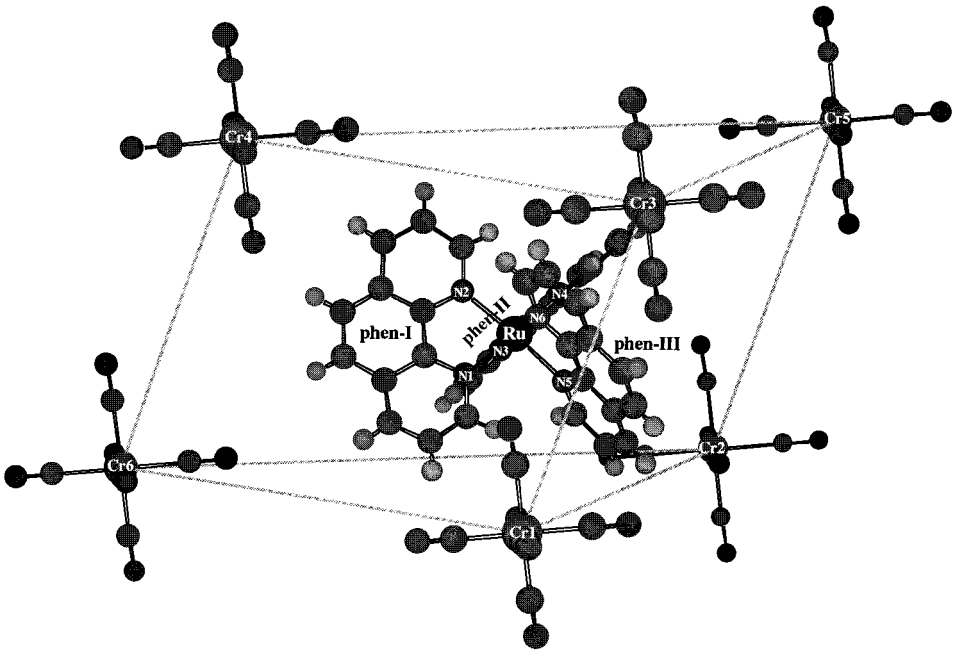

Figure 1. Relative position of $[Cr(CN)_6]^{3-}$ to $[Ru(phen)_3]^{2+}$ in $[Ru(phen)_3]_2[Cr(CN)_6]Cl\cdot2(CH_3)_2CO\cdot14H_2O$.

$(phen)_3]^{2+}$ in $[Ru(phen)_3]_2[Cr(CN)_6]Cl\cdot2(CH_3)_2CO\cdot14H_2O$ is very different from that in $[Ru(bpy)_3]_2[Cr(CN)_6]X\cdot8H_2O$. $[Ru(phen)_3]^{2+}$ in $[Ru(phen)_3]_2[Cr(CN)_6]Cl\cdot2(CH_3)_2CO\cdot14H_2O$ is found to have as its three nearest neighbors $[Cr(CN)_6]^{3-}$ within 10.2 Å (7.170, 9.190, and 10.190 Å), and three more within 13.1 Å (11.749, 12.805 and 13.053 Å). Figure 1 shows the relative molecular geometry of $[Cr(CN)_6]^{3-}$ surrounding $[Ru(phen)_3]^{2+}$ in $[Ru(phen)_3]_2[Cr(CN)_6]Cl\cdot2(CH_3)_2CO\cdot14H_2O$. The relative positions of the acceptor complexes $[Cr(CN)_6]^{3-}$ in relation to the donor complex $[Ru(phen)_3]^{2+}$ in $[Ru(phen)_3]_2[Cr(CN)_6]Cl\cdot2(CH_3)_2CO\cdot14H_2O$ are also very different from those in relation to $[Ru(bpy)_3]^{2+}$ in $[Ru(bpy)_3]_2[Cr(CN)_6]X\cdot8H_2O$. In Table 3, the distance and relative position parameter of the chromium(III) center and the $[Ru(N\text{-}N)_3]^{2+}$ are listed, where $|\boldsymbol{r}|$ represents the distance between ruthenium(II) and chromium(III) centers, θ is the angle between the *x*-axis and the projection of $\boldsymbol{r}$ to the x-y plane (the ligand bpy- or phen-plane), and ϕ is the elevation angle from the bpy- or phen-plane.[14,18] The six $[Cr(CN)_6]^{3-}$ around $[Ru(bpy)_3]^{2+}$ are located at equivalent positions relative to the donor complex in $[Ru(bpy)_3]_2[Cr(CN)_6]X\cdot8H_2O$. The two $[Cr(CN)_6]^{3-}$ are located in the direction of the 4- and 4′-carbon atoms of the bpy ligand; one is above the bpy-plane and the other is below it, respectively.[14] Figure 2(a) shows the relative geometry between $[Ru(bpy)_3]^{2+}$ and $[Cr(CN)_6]^{3-}$, whose distance is the shortest. In $[Ru(bpy)_3]_2[Cr(CN)_6]Cl\cdot8H_2O$, the chromium(III) ion is located in the direction of $|\theta| = 32.2°$ and $|\phi| = 15.5°$, and the Ru−Cr distance $|\boldsymbol{r}|$ is 9.173 Å for site-A ($|\theta| = 31.9°$, $|\phi| = 18.2°$, and $|\boldsymbol{r}| = 9.244$ Å for site-B). The 3-fold axis of the $[Cr(CN)_6]^{3-}$ points toward the ruthenium(II) ion. The other five chromium(III) ions are also the same relative position as the nearest one: $|\theta| = 26.0-36.6°$ (average = 31.6°), $|\phi| = 15.5-21.8°$ (average = 19.1°), and $|\boldsymbol{r}| = 9.173-9.883$ Å (average = 9.500 Å) for site-A; and $|\theta| = 27.0-35.2°$ (average = 31.5°), $|\phi| = 18.2-22.1°$ (average = 20.6°), and $|\boldsymbol{r}| = 9.244-9.883$ Å (average = 9.510 Å) for site-B. Thus, all the $[Cr(CN)_6]^{3-}$ are in the outer sphere of $[Ru(bpy)_3]^{2+}$, as shown in Figure 2(a). In contrast, $[Cr(CN)_6]^{3-}$ around $[Ru(phen)_3]^{2+}$ is located at the nonequivalent position relative to the donor complex in $[Ru(phen)_3]_2[Cr(CN)_6]Cl\cdot2(CH_3)_2CO\cdot14H_2O$. Figure 2(b) shows the relative geometry between $[Ru(phen)_3]^{2+}$ and $[Cr(CN)_6]^{3-}$, whose distance is the shortest. The nearest chromium(III) ion to a ruthenium(II) ion is located in the direction of $\theta = 88.3°$ and $\phi = 22.0°$ from phen-I (or $\theta = 26.0°$ and $\phi = 43.1°$ from phen-III) and at a distance of 7.170 Å from the ruthenium (II) ion. Thus, the $[Cr(CN)_6]^{3-}$ enters into the space of $[Ru(phen)_3]^{2+}$,

Table 3. Relative Geometry Parameter in $[Ru(bpy)_3]_2[Cr(CN)_6]Cl\cdot8H_2O$ and $[Ru(phen)_3]_2[Cr(CN)_6]Cl\cdot2(CH_3)_2CO\cdot14H_2O$

	ligand[a]	Cr[b]	$\lvert\boldsymbol{r}\rvert$, Å[c]	θ, deg[c]	ϕ, deg[c]	Cr−C, Å[d,e]
		$[Ru(bpy)_3]_2[Cr(CN)_6]Cl\cdot8H_2O$				
site-A	bpy-II (N3)	Cr6	9.393	28.0	17.7	4.871[d]
		Cr5	9.276	−36.6	−21.8	4.872[d]
	bpy-I (N2)	Cr2	9.883	32.0	19.0	5.433[d]
		Cr1	9.811	−26.0	−19.8	5.419[d]
	bpy-III (N4)	Cr4	9.465	34.8	21.0	5.080[d]
		Cr3	9.173	−32.2	−15.5	4.604[d]
	average		9.500	31.6	19.1	5.047[d]
site-B	bpy-II′ (N6)	Cr6	9.331	28.2	21.3	4.847[d]
		Cr5	9.319	−35.2	−20.2	4.905[d]
	bpy-I′ (N5)	Cr2	9.883	33.0	21.5	5.335[d]
		Cr1	9.872	−27.0	−20.3	5.454[d]
	bpy-III′ (N7)	Cr4	9.413	33.6	22.1	5.044[d]
		Cr3	9.244	−31.9	−18.2	4.727[d]
	average		9.510	31.5	20.6	5.050[d]
	$[Ru(phen)_3]_2[Cr(CN)_6]Cl\cdot2(CH_3)_2CO\cdot14H_2O$					
	phen−I	Cr1	7.170	88.3	22.0	4.698[e]
	(N1, N2)	Cr4	10.190	−35.0	4.7	5.372[e]
		Cr6	12.805	14.3	−25.8	8.263[e]
	phen-II	Cr2	11.749	9.6	33.0	7.919[e]
	(N3, N4)	Cr5	13.053	−40.3	8.0	8.320[e]
	phen-III	Cr1	7.170	26.0	43.1	4.959[e]
	(N5, N6)	Cr3	9.190	−45.0	−12.2	4.655[e]

[a] The figure after N is numbered the nitrogen atom of ligand-bpy or -phen in CIF file. [b] See Figure 1. [c] See ref 14 or 18. [d] The distance between the chromium(III) ion and the nearest carbon atom (4- or 4′-carbon atom) of ligand bipyridine from the chromium(III) ion. [e] The distance between the chromium(III) ion and the nearest carbon atom of ligand phenanthroline from the chromium(III) ion.

(18) See Figure S-4 in Supporting Information.

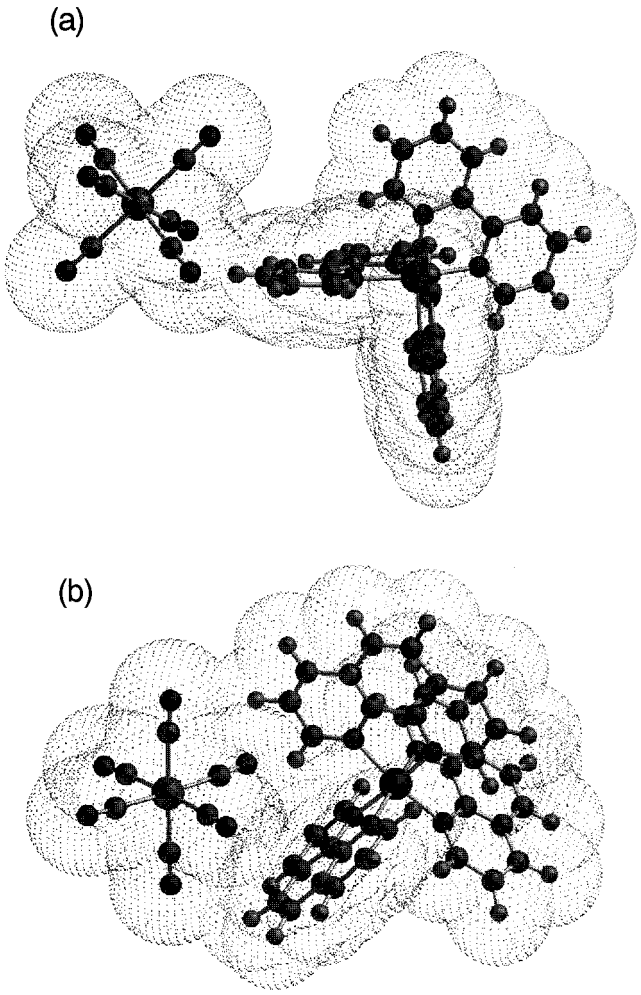

Figure 2. Molecular geometry of $[Ru(N\text{-}N)_3]^{2+}$ and $[Cr(CN)_6]^{3-}$ which are closest each other; (a) $[Ru(bpy)_3]_2[Cr(CN)_6]Cl\cdot 8H_2O$ (b) $[Ru(phen)_3]_2[Cr(CN)_6]Cl\cdot 2(CH_3)_2CO\cdot 14H_2O$.

as shown in Figure 2(b). A bisector of NC−Cr−CN (the 2-fold axis) in $[Cr(CN)_6]^{3-}$ points toward the ruthenium(II) ion. It is very surprising that the distance between the central metal ions of $[Ru(phen)_3]^{2+}$ and $[Cr(CN)_6]^{3-}$ (7.170 Å) is shorter by no less than 2 Å than that of $[Ru(bpy)_3]^{2+}$ and $[Cr(CN)_6]^{3-}$ (9.173 Å for site-A).

Absorption and Luminescence Spectra of $[Ru(N\text{-}N)_3]^{2+}$ and $[Cr(CN)_6]^{3-}$. The absorption and luminescence spectra of $[Ru(phen)_3]^{2+}$ are similar to those of $[Ru(bpy)_3]^{2+}$. The absorption band at 21 700 cm^{-1} and the luminescence band near 16 000 cm^{-1} are assigned to $^1A_1 \rightarrow {}^1$MLCT and ^{3}MLCT $\rightarrow {}^1A_1$, respectively (MLCT = metal-to-ligand charge-transfer excited state). The absorption bands of the acceptor $[Cr(CN)_6]^{3-}$ at 26 300 and 32 200 cm^{-1} are assigned to the spin-allowed $d-d^*$ transitions of $^4A_{2g} \rightarrow {}^4T_{2g}$ and $^4T_{1g}$, respectively. The luminescence band at 12 500 cm^{-1} is assigned to $^2E_g \rightarrow {}^4A_{2g}$. $[Ru(N\text{-}N)_3]^{2+}$ can absorb the light of the visible region, while $[Cr(CN)_6]^{3-}$ cannot.[14]

Luminescence and Excitation Spectra of Double-Complex Salts. Figure 3 shows the luminescence spectra of $[Ru(bpy)_3]_2[Cr(CN)_6]Cl\cdot 8H_2O$ and $[Ru(phen)_3]_2[Cr(CN)_6]Cl\cdot 2(CH_3)_2CO\cdot 14H_2O$ at 77 K irradiated at 21 700 cm^{-1} (460 nm). Both double-complex salts emit from not only $[Ru(N\text{-}N)_3]^{2+}$, but also $[Cr(CN)_6]^{3-}$. When the double-complex salts composed of $[Ru(N\text{-}N)_3]^{2+}$ and $[Cr(CN)_6]^{3-}$ are irradiated with light of the visible region, the $[Ru(N\text{-}N)_3]^{2+}$ can be excited selectively. Since the luminescence of $[Cr(CN)_6]^{3-}$ in a crystal of $K_3[Cr(CN)_6]$ is

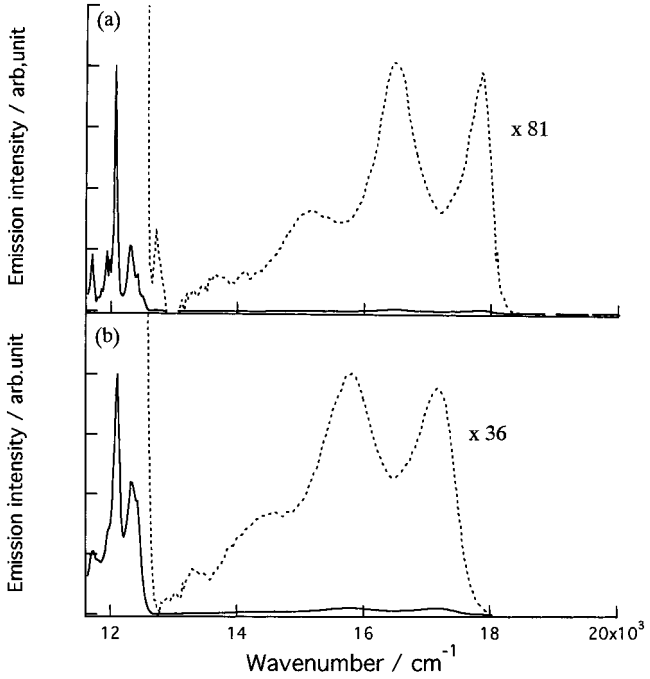

Figure 3. Luminescence spectra of double-complex salts at 77 K (excited at 21 700 cm^{-1}); (a) $[Ru(bpy)_3]_2[Cr(CN)_6]Cl\cdot 8H_2O$ (b) $[Ru(phen)_3]_2[Cr(CN)_6]Cl\cdot 2(CH_3)_2CO\cdot 14H_2O$.

hardly observed by irradiation at 21 700 cm^{-1} at 77 K, the luminescence from $[Cr(CN)_6]^{3-}$ in the double-complex salts can be assigned to the enhanced luminescence by the energy transfer from $[Ru(N\text{-}N)_3]^{2+}$ to $[Cr(CN)_6]^{3-}$. This energy transfer is also supported by the excitation spectra. Figure 4 shows the luminescence and excitation spectra of $[Ru(phen)_3]Cl\cdot 6H_2O$, $K_3[Cr(CN)_6]$, and $[Ru(phen)_3]_2[Cr(CN)_6]Cl\cdot 2(CH_3)_2CO\cdot 14H_2O$ at 77 K. The excitation spectrum monitored at the luminescence maximum of $[Cr(CN)_6]^{3-}$ in the crystal of $[Ru(phen)_3]_2[Cr(CN)_6]Cl\cdot 2(CH_3)_2CO\cdot 14H_2O$ (dotted line in Figure 4(c)) is similar to that of $[Ru(phen)_3]Cl\cdot 6H_2O$ (dotted line in Figure 4(a)), and it is very different from that of $K_3[Cr(CN)_6]$ (dotted line in Figure 4(b)). The same results can be obtained with regard to $[Ru(bpy)_3]_2[Cr(CN)_6]X\cdot 8H_2O$.[14]

Luminescence Lifetime and Energy-Transfer Rate. The emission intensity from $[Cr(CN)_6]^{3-}$ in $[Ru(phen)_3]_2[Cr(CN)_6]Cl\cdot 2(CH_3)_2CO\cdot 14H_2O$ is much smaller than that in $[Ru(bpy)_3]_2[Cr(CN)_6]Cl\cdot 8H_2O$. In contrast, the luminescence intensity from $[Ru(N\text{-}N)_3]^{2+}$ in the former salt is larger than that in the latter one. These results indicate that the yield of energy transfer in the former salt would be much smaller than that in the latter salt. The lifetime of the ^{3}MLCT state of $[Ru(N\text{-}N)_3]^{2+}$ in various crystals is summarized in Table 4. All decay curves at 77 K are single exponential.[19] Since the luminescence lifetimes of $[Ru(N\text{-}N)_3]^{2+}$ in the single- and double-complex salts where energy transfer cannot occur are almost constant at 77 K (3.6−6.0 μs), the rate constant of energy transfer (k_{ET}) can be evaluated using the luminescence lifetime of the energy donor from eq 1:

$$k_{ET} = 1/\tau_M - 1/\tau'_M \qquad (1)$$

where τ_M and τ'_M represent the lifetimes of donor $[Ru(N\text{-}N)_3]^{2+}$ in salts where energy transfer can occur and cannot occur, respectively.[9,14−16] The lifetime of $[Ru(phen)_3]^{2+}$ in $[Ru(phen)_3]_2[Cr(CN)_6]Cl\cdot 2(CH_3)_2CO\cdot 14H_2O$ can be estimated to

(19) See Figure S−5 in Supporting Information.

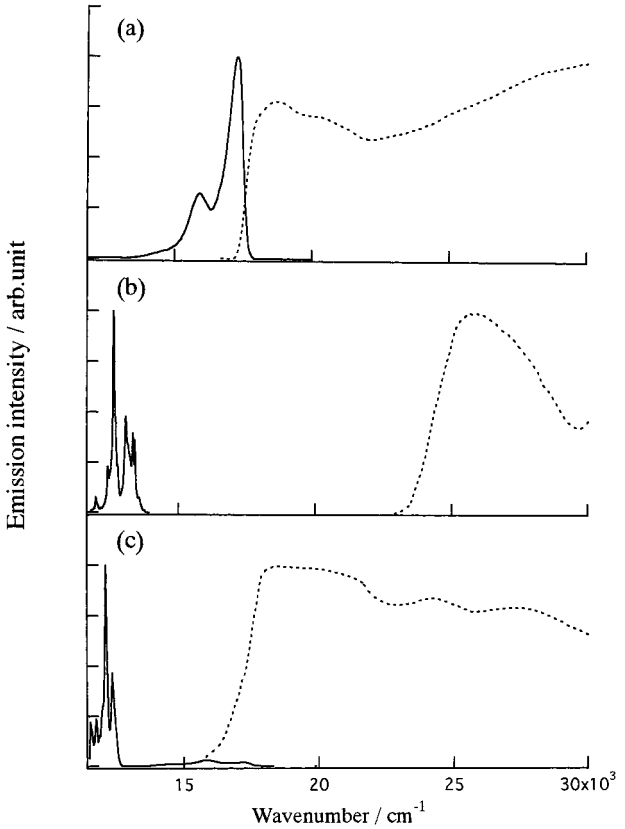

Figure 4. Luminescence (solid line) and excitation spectra (dot line) of the crystals at 77 K; (a) $[Ru(phen)_3]Cl_2 \cdot 6H_2O$ (monitored at 16 100 cm^{-1}), (b) $K_3[Cr(CN)_6]$ (monitored at 12 300 cm^{-1}), and (c) $[Ru(phen)_3]_2[Cr(CN)_6]Cl \cdot 2(CH_3)_2CO \cdot 14H_2O$ (monitored at 12 300 cm^{-1}).

Table 4. Lifetime and Decay Rate of ^{3}CT State of $[Ru(N\text{-}N)_3]^{2+}$ (N-N = bpy, phen) and Estimated Rate Constant of Energy Transfer (k_{ET}) in Various Crystals at 77 K

sample	lifetime, ns	decay rate, $10^6\ s^{-1}$	k_{ET}, $10^6\ s^{-1}$
$[Ru(bpy)_3]_2[Cr(CN)_6]Cl \cdot 8H_2O$	160	6.3	6.0
$[Ru(phen)_3]_2[Cr(CN)_6]Cl \cdot 2(CH_3)_2CO \cdot 14H_2O$	890	1.1	0.95
$[Ru(bpy)_3]Cl_2 \cdot 6H_2O$	5500	0.18	
$[Ru(bpy)_3]SO_4 \cdot 8H_2O$	3800	0.26	
$[Ru(bpy)_3]I_2 \cdot 6H_2O$	3600	0.28	
$[Ru(bpy)_3]_2[Co(CN)_6]Cl \cdot 8H_2O$	5900	0.17	
1%Ru^{2+}: $[Zn(bpy)_3]_2[Co(CN)_6]Cl \cdot 8H_2O$	5900	0.17	
$[Ru(phen)_3]Cl_2 \cdot 6H_2O$	6000	0.17	
$[Ru(phen)_3]SO_4 \cdot 10H_2O$	6000	0.17	

be about 890 ns. This lifetime is much longer than that of $[Ru(bpy)_3]^{2+}$ in $[Ru(bpy)_3]_2[Cr(CN)_6]Cl \cdot 8H_2O$ (160 ns). The energy migration between the donor's complexes in the salts does not contribute to the observed luminescence lifetime because the donor's lifetime in a pure crystal is much the same as that in a doped crystal $[M_{0.01}Zn_{0.99}(bpy)_3]_2[Cr(CN)_6]Cl \cdot 8H_2O$ (M^{2+} = Ru^{2+}, Os^{2+}).[14] At 77 K, the thermally activated pathway of the intramolecular transition from the ^{3}MLCT state (Ru^{2+}) to the ^{3}metal-center state (Ru^{2+}) is ignored; it is not important because the temperature is too low to bring about the transition.[14] The energy-transfer rates were estimated using eq 1, where 5 900 ns is used as τ'_M in this work. The obtained rate constants are also listed in Table 4. The rate constant of energy transfer in $[Ru(phen)_3]_2[Cr(CN)_6]Cl \cdot 2(CH_3)_2CO \cdot 14H_2O$ ($9.5 \times 10^5\ s^{-1}$) is one-order smaller than that in $[Ru(bpy)_3]_2[Cr(CN)_6]Cl \cdot 8H_2O$ ($6.0 \times 10^6\ s^{-1}$). This result is particularly surprising in view of the fact that the distance between the central metal ions of ruthenium(II) and chromium(III) complexes in $[Ru(phen)_3]_2[Cr(CN)_6]Cl \cdot 2(CH_3)_2CO \cdot 14H_2O$ is about 2 Å shorter than the distance in $[Ru(bpy)_3]_2[Cr(CN)_6]Cl \cdot 8H_2O$. It is noted that, in aqueous solutions, the quenching rate constants (k_q) of the luminescence of $[Ru(N\text{-}N)_3]^{2+}$ by $[Cr(CN)_6]^{3-}$ are comparable at 298 K; for example, $k_q = 4.40 \times 10^9\ M^{-1}\ s^{-1}$ for $[Ru(phen)_3]^{2+}$ and $3.97 \times 10^9\ M^{-1}\ s^{-1}$ for $[Ru(bpy)_3]^{2+}$ at 0.04 M ionic strength.[20]

Relationship between Crystal Structure and Energy-Transfer Rate. The energy-transfer rate constant depends mainly upon the following three factors: (i) distance between the donor and the acceptor, (ii) spectral overlap between the donor's luminescence spectrum and the acceptor's absorption spectrum, and (iii) relative orientation between the donor and the acceptor.[14] In this study, the spectral overlaps are similar for $[Ru(phen)_3]_2[Cr(CN)_6]Cl \cdot 2(CH_3)_2CO \cdot 14H_2O$ and $[Ru(bpy)_3]_2[Cr(CN)_6]Cl \cdot 8H_2O$ since the luminescence spectrum from the ^{3}MLCT state of $[Ru(phen)_3]^{2+}$ is almost the same as that of $[Ru(bpy)_3]^{2+}$ (see Figure 3). The results of X-ray structure analysis show that the distance between the centers of the donor and the acceptor in $[Ru(phen)_3]_2[Cr(CN)_6]Cl \cdot 2(CH_3)_2CO \cdot 14H_2O$ is about 2 Å shorter than that in $[Ru(bpy)_3]_2[Cr(CN)_6]Cl \cdot 8H_2O$ (see Table 3). Under this condition, it is expected that the energy-transfer rate constant in the former salt would be much larger than that in the latter salt based on the short distance and the same spectral overlap. However, the experimental results obtained in this work are the opposite of those expected. Therefore, these results indicate that the energy-transfer rate constant in the double-complex salts does depend on factor (iii), which is the relative orientation between donor and acceptor.

We consider the orientation of $[Ru(N\text{-}N)_3]^{2+}$ and $[Cr(CN)_6]^{3-}$, which are the closest each other. Figure 2 shows the molecular geometry of $[Ru(N\text{-}N)_3]^{2+}$ and $[Cr(CN)_6]^{3-}$. In $[Ru(bpy)_3]_2[Cr(CN)_6]Cl \cdot 8H_2O$, where the energy transfer can occur effectively, the Cr atom is located in the direction of $|\theta| = 32.2°$ and $|\phi| = 15.5°$ to $[Ru(bpy)_3]^{2+}$ and at 9.173 Å from the Ru atom (for site-A). In other words, the Cr atom is located in the direction of the 4-carbon atom of bpy from the Ru atom, and the elevated angle ($|\phi|$) of the Cr−(Ru−bpy plane) is 15.5°. A 3-fold axis of $[Cr(CN)_6]^{3-}$ points toward the Ru atom. On the other hand, in $[Ru(phen)_3]_2[Cr(CN)_6]Cl \cdot 2(CH_3)_2CO \cdot 14H_2O$, where a small amount of energy transfer occurs, the Cr atom is located in the direction of $|\theta| = 88.3°$ and $|\phi| = 22.0°$ from phen-I (or $|\theta| = 26.0°$ and $|\phi| = 43.1°$ from phen-III) and at 7.170 Å from the Ru atom. The Cr atom is located in the space between two phen ligands of $[Ru(phen)_3]^{2+}$. A bisector of NC−Cr−CN in $[Cr(CN)_6]^{3-}$ points toward the Ru atom (see Figure 2).

In consideration of these results together, it is concluded that the energy absorbed by $[Ru(bpy)_3]^{2+}$ can transfer effectively to the $[Cr(CN)_6]^{3-}$ located in the direction of the 4-carbon atom of the bpy ligand and within 10 Å from the Ru atom in $[Ru(bpy)_3]_2[Cr(CN)_6]Cl \cdot 8H_2O$, while the energy absorbed by $[Ru(phen)_3]^{2+}$ can transfer ineffectively to the $[Cr(CN)_6]^{3-}$, entering the space between two phen ligands of $[Ru(phen)_3]^{2+}$ in $[Ru(phen)_3]_2[Cr(CN)_6]Cl \cdot 2(CH_3)_2CO \cdot 14H_2O$, even if the distance between the Ru and Cr atoms is shorter than that in $[Ru(bpy)_3]_2[Cr(CN)_6]Cl \cdot 8H_2O$ by 2 Å.

Energy Transfer Mechanism. In general, two energy transfer mechanisms have been proposed.[21] One is called the Dexter mechanism, in which energy transfer can occur by

(20) Iwamura, M.; Otsuka, T.; Kaizu, Y., submitted for publication.
(21) *Energy Transfer Processes in Condensed Matter*; Di Bartolo, B., Ed.; Plenum Press: New York, 1984.

electron exchange interaction.[22,23] The other is the Förster mechanism, in which the transfer is brought about by a dipole−dipole interaction.[24−27]

In the double-complex salts of $[M(bpy)_3]_2[Cr(CN)_6]Cl\cdot 8H_2O$ ($M^{2+} = Ru^{2+}$, Os^{2+}), it is concluded that the energy transfer is brought about by the Dexter mechanism.[14] This is because (i) the spectrum of the donor's luminescence overlaps negligibly with that of the acceptor's absorption, because the energy of the maximum luminescence of donor (about 570 nm) is very different from that of the absorption maximum of the acceptor (about 800 nm), and the acceptor's absorption band, ^2E_g, is very narrow, and (ii) the molar extinction coefficient of the ^2E_g state of $[Cr(CN)_6]^{3-}$ is enormously small (about 0.1 M^{-1} cm^{-1}). The distance between the Cr atom to the carbon atom of the bpy ligand is less than 5 Å (4.604 Å) although the Ru−Cr distance is more than 9 Å (9.173 Å), therefore, it is reasonable that the d-orbital of Cr(III) ion overlaps with the π-orbital of the bpy ligand.

The intermolecular energy transfer in $[Ru(phen)_3]_2[Cr(CN)_6]Cl\cdot 2(CH_3)_2CO\cdot 14H_2O$ should also be brought about by the Dexter mechanism, since this system also possesses the same conditions of (i) and (ii), and the distance between the Cr atom to the carbon atom of the phen ligand is also less than 5 Å (4.655 Å), although the relative geometry is not suitable for effective energy transfer.

Concluding Remarks

Based on X-ray structure analysis, the distance between the Ru and Cr atoms in $[Ru(phen)_3]_2[Cr(CN)_6]Cl\cdot 2(CH_3)_2CO\cdot 14H_2O$ (7.170 Å) is about 2 Å shorter than that in $[Ru(bpy)_3]_2[Cr(CN)_6]Cl\cdot 8H_2O$ (9.173 Å). However, the rate constant of energy transfer in the former salt (9.5×10^5 s^{-1}) is far smaller than that in the latter salt (6.0×10^6 s^{-1}). These results indicate that the energy transfer strongly depends on the relative orientation between the donor and the acceptor in the double-complex salts. It is suggested that energy transfer can occur easily when the chromate(III) complex is located in the direction of the 4-carbon atom of the bpy ligand in $[Ru(bpy)_3]_2[Cr(CN)_6]Cl\cdot 8H_2O$, while the transfer occurs less efficiently when the chromate(III) complex enters the space between the planes of the phen ligand of $[Ru(phen)_3]^{2+}$ in $[Ru(phen)_3]_2[Cr(CN)_6]Cl\cdot 2(CH_3)_2CO\cdot 14H_2O$, even if the distance between the Ru and Cr atoms is shorter than that in $[Ru(bpy)_3]_2[Cr(CN)_6]Cl\cdot 8H_2O$ by 2 Å.

Acknowledgment. The present work was partially supported by a Grant-in-Aid for Encouragement of Young Scientists No. 12740359 from the Ministry of Education, Science, and Culture of Japan.

Supporting Information Available: Figures of the ORTEP drawings, the relative orientation parameters and the luminescence decay curves of $[Ru(N\text{-}N)_3]^{2+}$ in the double-complex salts, and X-ray crystallographic files, in CIF and PDF formats, are available free of charge via the Internet at http://pubs.acs.org.

IC0013936

(22) Dexter, D. L. *J. Chem. Phys.* **1953**, *21*, 836.
(23) Lamola, A. A. In *Energy transfer and Organic Photochemistry*; Lamola, A. A., Turro, N. J., Eds.; Interscience: New York, 1969; p 17.
(24) Förster, T. *Ann. Phys.* **1948**, *2*, 55.
(25) Förster, T. *Z. Elektrochem.* **1949**, *53*, 93.
(26) Förster, T. *Fluoresezenz organische Verbindungen*; Vandenhoecck and Ruprecht: Göttingen, 1951.
(27) Förster, T. *Discuss. Faraday Soc.* **1959**, *27*, 7.